Chemical Physics 83 (1984) 133–146
North-Holland, Amsterdam

ROLE OF TRANSLATIONAL–ROTATIONAL COUPLING IN LATTICE DYNAMICS AND FERROELASTIC PHASE TRANSITIONS; THE s-TRIAZINE CRYSTAL

Tadeusz LUTY

Institute of Organic and Physical Chemistry, Technical University, Wrocław, Poland

and

Ad VAN DER AVOIRD

Institute of Theoretical Chemistry, University of Nijmegen, Nijmegen, The Netherlands

Received 23 June 1983

An analysis of the lattice dynamics for low- and high-temperature phases of s-triazine crystals is presented. Special attention is paid to the problem of translational–rotational coupling as a driving force for the structural phase transition. Results of numerical calculations for static and dynamical properties are used to predict parameters of the Landau free-energy expansion for the crystal. Finally, recent theories of the ferroelastic phase transition in the s-triazine crystal are critically discussed.

1. Introduction

It has long been known that in molecular crystals there should be a coupling between rotations and translations of molecules. This coupling follows naturally from the distance and orientation dependence of the intermolecular potential. Recently, one can notice an extensive interest in theoretical [1] and experimental [2] aspects of translational–rotational coupling, mostly in a relation to ferroelastic, orientational phase transitions in molecular crystals. So far, the attention has been focused on "semimolecular", ionic crystals like KCN and NH_4Cl, where the reorientational motions of the molecular ions couple to acoustic phonons. As a result of this coupling, drastic thermoelastic anomalies appear, which can be observed as a striking lowering of the elastic stiffness near phase-transition temperatures. Crudely speaking, the molecular ions in that type of crystals play a role of "molecular grease", lowering the response of the crystal to shear strain. This role is evident from experiments with doped crystals KCl : KCN, where a decrease of the sound velocity by an appreciable amount has been found [3] as a consequence of doping.

The theoretical approach to the translational–rotational coupling in "semimolecular" crystals, worked out by Michel and Naudts [4], although quite complicated, is not a general one. In the theory, microscopic in principle, but phenomenological in fact, direct rotational coupling between molecules is neglected and a molecule feels a mean rotational field. The theory is limited to the case of highly orientationally disordered crystals with one molecule in the unit cell. For such crystals it predicts rotational coupling between molecules as due to indirect interactions, mediated by acoustic phonons via translational–rotational coupling. It has to be emphasized that for these crystals an effective rotational interaction is responsible for the rotational phase transition (freezing of CN^- ion orientations in the KCN crystal, for example) which is accompanied by a structural phase transition (unit-cell deformation).

On the other hand, not too much attention has been devoted to translational–rotational coupling and its manifestation in crystal properties of less

anharmonic molecular crystals, where librational motions can still be considered as well localized. These systems are simpler in principle. Examples are the recently well-studied crystals of s-triazine [5] and benzil [6], where a coupling between unit-cell deformations and molecular rotations is clearly observed and ferroelastic phase transitions occur. These observations suggested us to look for a microscopic, lattice dynamical, description of the static and dynamical consequences of translational–rotational coupling in crystals where librational and acoustic phonons are still well-defined excitations.

The crystal of s-triazine is a good example to illustrate the role of translational–rotational coupling in the structural phase transition, for which an effective translational potential could be held responsible. A weak first-order transition in s-triazine crystals occurs at ≈ 200 K, from a high-temperature trigonal phase (space group $R\bar{3}c$) to a low-temperature monoclinic phase (space group $C2/c$). The anomalous thermoelastic properties of the crystal [5,7] have been interpreted in terms of a coupling between the shear strain component, $e_4 = e_5$, and molecular rotations (R_x, R_y). A phenomenological theory of the transition based on the mean-field approximation has been presented by Raich and Bernstein [8] but it has been criticized recently by Rae [9]. In order to clarify some of the contradictory points of the discussion [10], a detailed lattice dynamical analysis, even within the conventional harmonic approximation, seems to be helpful.

The aim of this paper is to analyze the statics and dynamics of the s-triazine lattice, to relate it to the phenomenological theories of the phase transition and, also, to the correlation-function approach [11,12]. It is too much to say that the paper offers a microscopic model for the phase transition, although the calculations presented here do predict parameters of the conventional Landau theory, which is a requirement for any microscopic model [13].

We start with a description of crystal structures of s-triazine and the potential for intermolecular interactions. In section 3, results of lattice dynamics calculations for the high-temperature phase are presented and a detailed analysis of the influence of translational–rotational coupling on the elastic constants (acoustic phonons) is performed. These considerations are then related to the free-energy expansion in terms of strain, e_4, and molecular rotation, R_y, and parameters of this expansion are calculated in section 4. Numerically simulated shear strain allows us to calculate the lattice dynamics of the low-temperature, monoclinic phase and the results are presented in section 5. Finally, in section 6 an interpretation of the phase transition, based on the lattice dynamical calculations, is presented; a critical comparison with previously suggested models is made.

2. Statics of the s-triazine crystal

2.1. Crystal structures

The crystal structures of s-triazine are well known from X-ray diffraction [14]. In the high-temperature, trigonal phase ($R\bar{3}c$) the molecules form infinite stacks along the hexagonal axis c and the nearest molecules, within the stack, are related by a center of inversion. The structure is schematically shown in fig. 1. It is convenient to represent the structure as pseudo-orthorhombic (see ref. [14]) or, what is preferred here, as a pseudo-monoclinic one. The relation between these structures is also shown in fig. 1 and the monoclinic unit-cell parameters can be expressed as

$$a_m^0 = \left(\tfrac{1}{3}a_h^2 + \tfrac{4}{9}c_h^2\right)^{1/2}, \quad b_m^0 = a_h, \quad c_m^0 = c_h,$$
$$\beta_m^0 = \tfrac{1}{2}\pi + \tan^{-1}\left(2c_h/3^{1/2}a_h\right). \qquad (1)$$

The monoclinic representation of the high-temperature crystal structure is especially convenient in a discussion of the phase transition to the low-temperature monoclinic phase. The phase transition at ≈ 200 K is followed by a deformation of the high-temperature unit cell, accompanied by a tilt of the molecules. Actually, the symmetry of the low-temperature phase ($C2/c$) allows the tilt to be accompanied additionally by a translational displacement of the molecules along the rotation axis, in such a way that the center of inversion, which relates two nearest molecules within the stack, is preserved. It is well known that the s-tri-

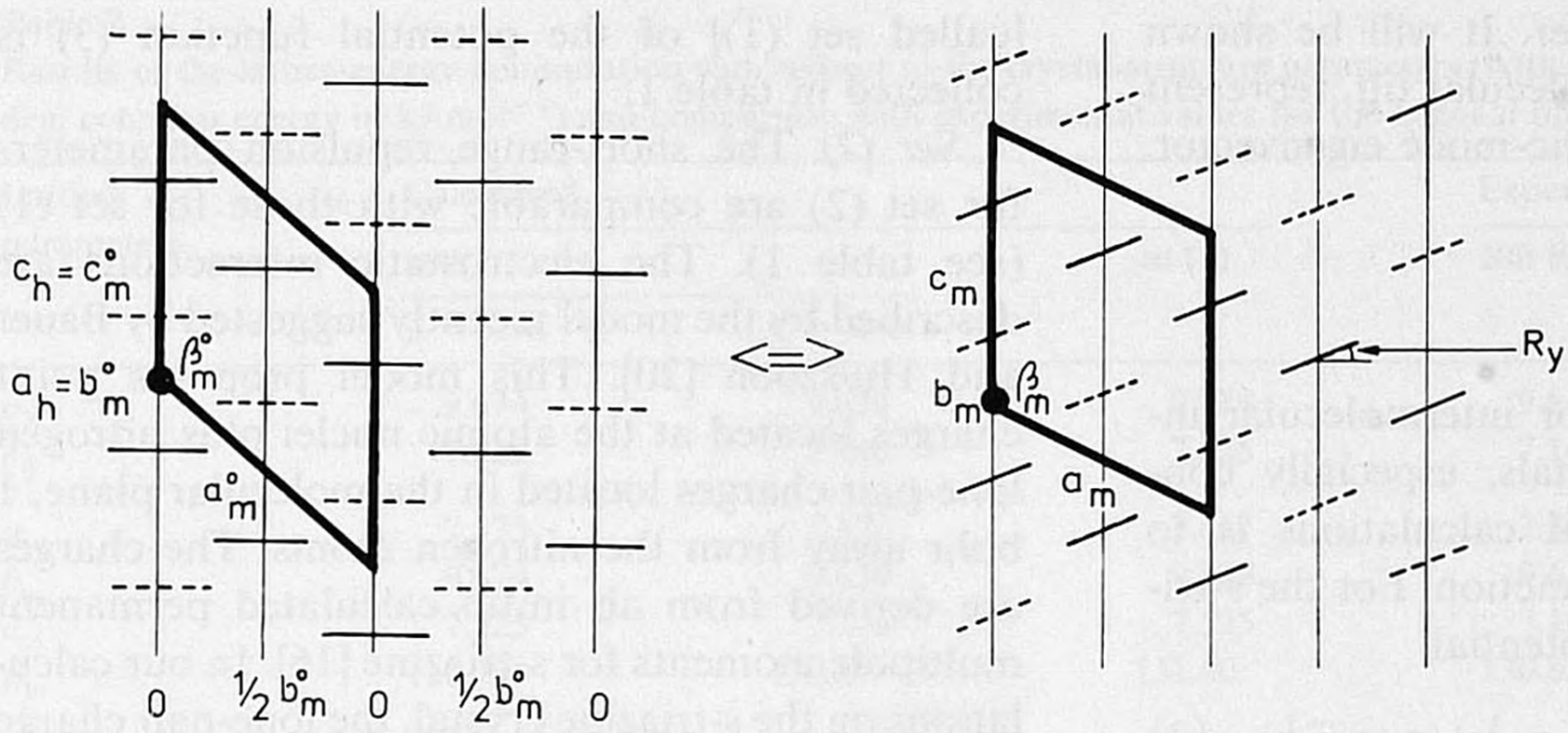

Fig. 1. Schematic projection of the crystal structure of s-triazine on the (010) plane for high-temperature (left) and low-temperature (right) phases. The monoclinic representation of the structures is indicated.

azine crystal develops three domains below the transition temperature [14]. However, for a more transparent picture and without loss of generality we shall concentrate on one domain, in which the shear strain component, e_4, and the molecular rotation R_y are the order parameters. The parameters are defined in the orthogonal axis system x, y, z, assigned to the crystal axis system a'_m, b_m, c_m. A schematic structure of the low-temperature phase is also shown in fig. 1. The strain component, e_4, which for symmetry reasons has to be zero in the trigonal phase, can be related to the lattice parameters [15]:

$$e_4 = \cot \beta_m - \cot \beta_m^0, \tag{2}$$

where β_m^0 is the monoclinic angle of the trigonal phase given by relation (1). It is clear that the shear strain component can be treated as an order parameter for the structural phase transition and its temperature dependence indicates the transition to be weakly first order [14]. On the other hand, the orientation of the molecules in the high-temperature phase is fixed by the crystal symmetry and so the tilt of the molecules can equally well be

Table 1
Two sets of parameters of the site–site "6-exp-1" potential function used for the s-triazine crystal

Contact $i \cdots j$	A_{ij} (kJ mol^{-1} Å^6) both sets	B_{ij} (kJ mol^{-1})		C_{ij} (Å^{-1})	
		set (1)	set (2)	set (1)	set (2)
C ··· C	2720.0	311498.0	311498.0	3.38	3.36
C ··· H	552.0	39400.0	72122.0	3.67	3.53
C ··· N	2395.0	184948.0	184948.0	3.38	3.36
H ··· H	113.0	16699.0	16699.0	3.74	3.74
H ··· N	485.0	23500.0	42820.0	3.56	3.55
N ··· N	2107.0	109808.0	109808.0	3.38	3.36
Charges [a] q_i	q_C	q_N	q_H	q_{lp}	
set (1)	0.135	−0.170	0.035	–	
set (2)	−0.22	0.69	0.22	−0.69	

[a] In unit charges $e = 1.602 \times 10^{19}$ C.

treated as an order parameter. It will be shown that both, shear strain and molecular tilt, represent a frozen pattern of an acoustic-mode eigenvector.

2.2. Intermolecular potential

A useful approximation for intermolecular interactions in molecular crystals, especially convenient for lattice dynamical calculations is to assume a site–site potential function. For the s-triazine crystal the "6-exp-1" potential

$$V_{ij} = -A_{ij} r_{ij}^{-6} + B_{ij} \exp(-C_{ij} r_{ij}) + q_i q_j r_{ij}^{-1}, \quad (3)$$

has been chosen to represent the interactions between ith and jth sites of different molecules. The calculations are carried out with two sets of potential parameters. The dispersion interaction parameters, A_{ij}, have been taken from the work by Mulder et al. [16] and they are the same for both sets.

Set (1) The short-range repulsion parameters, B_{ij}, were the same as used by Rae [17] and the exponential parameters, C_{ij}, for C ··· C, C ··· N and N ··· N contacts have been assumed to be equal; the latter were finally taken as a fit parameter. In this set the electrostatic part of the potential is described by interactions between net atomic charges located at the nuclei. The information about the charges has been taken from an electron-density analysis for the s-triazine crystal [18]. This analysis yields the following net charges: $q_C = 0.19\ e$, $q_N = -0.24\ e$ and $q_H = 0.05\ e$. When these charges were used to calculate the crystal energy as a sum of pair potentials (3), the energy minimum was found far from the experimental structure. In order to reproduce the crystal structure in the high-temperature phase, it was decided to fit the parameter $C = C_{CC} = C_{CN} = C_{NN}$ and the atomic charges, keeping the ratio $q_C : q_N : q_H$ as found from the valence-density analysis [18]. After few minimization runs [19], the atomic charges $q_C = 0.135\ e$, $q_N = -0.170\ e$, $q_H = 0.035\ e$ and the parameter $C = 3.40/3.38$ Å^{-1} have been found. For the higher value of C, the structure is close to the experimental one at ≈ 200 K, while for the value of 3.38 Å^{-1} the trigonal structure at 300 K is closely reproduced. The final set of parameters [called set (1)] of the potential function (3) is collected in table 1.

Set (2) The short-range repulsion parameters for set (2) are comparable with those for set (1) (see table 1). The electrostatic interactions are described by the model recently suggested by Bauer and Huiszoon [20]. This model proposes point charges located at the atomic nuclei plus nitrogen lone-pair charges located in the molecular plane, 1 bohr away from the nitrogen atoms. The charges are derived from ab initio calculated permanent multipole moments for s-triazine [16]. In our calculations on the s-triazine crystal, the lone-pair charge location has been shifted closer to nitrogen, at a distance of 0.1 Å, keeping the nitrogen–lone-pair dipole moment constant at 0.365 e Å. This appears to work better, probably because there is no explicit lone-pair repulsion term in the potential (3). A shorter lone-pair distance was actually recommended in ref. [20]. The parameters of set (2) are also collected in table 1.

Results of the crystal-structure optimizations with both sets of parameters are presented in table 2. It has to be emphasized that the minimization of the lattice energy (forty-two nearest-neighbour molecules included) has been performed with respect to the unit-cell parameters: a_m, b_m, c_m, β_m and two parameters, R_y and T_y, describing molecular rotation about and translation along the $y = b_m$ axis. This set of variables allowed us in principle to obtain the trigonal as well as the monoclinic (low-temperature) structure as a result of the lattice-energy minimization. Actually, all minimization runs for both parameter sets gave the high-temperature trigonal structure. Although the set (2) seems to be better justified it gives slightly worse results for the lattice constants, as compared with the experimental ones. The results of our calculations cannot be directly compared with recent calculations by Gamba and Bonadeo [21], as these authors *did not* minimize the crystal potential with respect to the unit-cell parameters. Thus it is not clear whether the potential suggested in ref. [21] gives a minimum close to the experimental structure and, thus whether it is theoretically justified to perform lattice dynamical calculations with this potential for the observed structure.

An additional criterion for the quality of the

Table 2
Results of the lattice-energy minimization with respect to the crystal-structure parameters (lattice constants in Å, monoclinic angle in deg, cohesion energy in kJ mol^{-1}) and comparison with experimental values for the trigonal phase of s-triazine

Lattice parameters	Calculated			Experimental [14,21]	
	set (1)		set (2)	200 K	300 K
	$C = 3.38$	$C = 3.40$			
a_h	9.674	9.639	9.788	9.619	9.647
c_h	7.225	7.146	7.525	7.149	7.281
a_m	7.375	7.326	7.557	7.318	7.388
b_m	9.674	9.639	9.788	9.619	9.647
c_m	7.225	7.146	7.525	7.149	7.281
β_m	130.78	130.57	131.60	130.63	131.07
cohesion energy	65.7	67.6	47.7	47.7	

potential for the s-triazine crystal is the comparison of calculated and experimental dynamical properties of the crystal and this is done in the next section.

3. Lattice dynamics of the trigonal phase

The lattice dynamics of the s-triazine crystal has been solved for the equilibrium, trigonal structures, which are reasonably close to the experimental ones for both sets of the potential parameters. The force-constant matrices for forty-two nearest molecules have been calculated and the dynamical matrix $\mathbf{D}(\boldsymbol{q})$ (12×12) constructed. Finally, the secular equation

$$\left[\mathbf{D}(\boldsymbol{q}) - \mathbf{M}\omega^2(\boldsymbol{q})\right] V(\boldsymbol{q}) = 0, \qquad (4)$$

with the mass-tensor $\mathbf{M}$ has been solved for two symmetry directions $[q_x, 0, 0]$ and $[0, 0, q_z]$. The dispersion curves as calculated with parameter set (1) and the symmetry assignments are shown in fig. 2. The optical phonons at the center of the Brillouin zone and the acoustic phonons in the indicated symmetry directions will be discussed in some detail as they are related to the phase transition in the crystal.

3.1. Zone-center optical phonons

At the center of the Brillouin zone for the trigonal phase there are nine optical phonons which can be classified according to irreducible representations of the D_{3d} point group: $2\,A_{2g} + 2\,E_g + A_{2u} + E_u$. As it follows from the group theoretical analysis, the "ungerade" modes correspond to

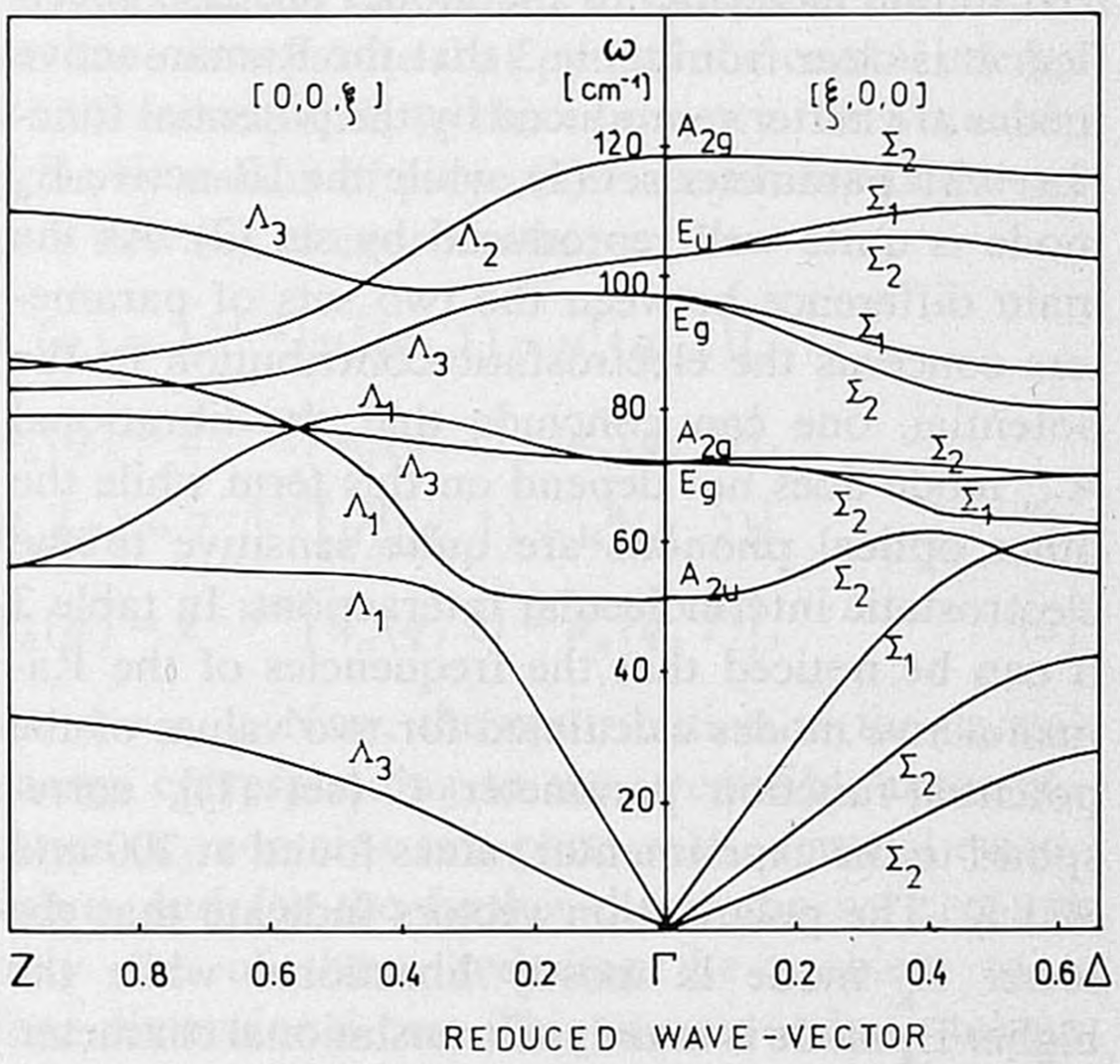

Fig. 2. Phonon-dispersion curves for two symmetry directions of the trigonal phase of s-triazine.

Table 3
Optical-phonon frequencies (in cm^{-1}) at $\boldsymbol{q} = 0$ and their polarization vectors (normalized to one molecule for parameter set (1) with $C = 3.40$ $Å^{-1}$) calculated for the trigonal phase of s-triazine and compared with available experimental values

Mode	Calculations									Experiment [a]	
	set (2)	set (1)		polarization vectors						200 K	300 K
		$C = 3.38$	$C = 3.40$	T_x	T_y	T_z	R_x	R_y	R_z		
A_{2u}	48.9	48.9	50.8	0	0	0	0	0	1.0	–	–
E_g	78.6	69.5	71.5	−0.43	0	0	−0.90	0	0	71.0	68.0
				0	0.43	0	0	0.90	0		
A_{2g}	90.1	71.0	72.0	0	0	0.28	0	0	0.97	–	–
E_g	103.5	94.5	96.7	−0.90	0	0	0.43	0	0	98.0	92.0
				0	−0.90	0	0	0.43	0		
E_u	89.4	99.0	102.7	0	0	0	1.0	0	0	–	84.0
				0	0	0	0	1.0	0		
A_{2g}	121.8	114.9	118.2	0	0	−0.97	0	0	−0.28	–	–

[a] For the Raman-active modes, the values are taken from ref. [22], and for the IR-active mode from ref. [23].

purely librational vibrations, while the "gerade" ones are of mixed translational–rotational character. This is a result of the crystal symmetry that includes a center of inversion which relates two translationally non-equivalent molecules in the primitive unit cell.

In table 3 the calculated frequencies of the optical phonons are compared with experimental values [22,23]. The polarization vectors (normalized to one molecule) of the modes are also specified. It is clear from table 3 that the Raman-active modes are better reproduced by the potential function with parameter set (1), while the IR-active E_u mode is quite well reproduced by set (2). As the main difference between the two sets of parameters concerns the electrostatic contribution to the potential, one can conclude that the librational A_{2u} mode does not depend on this term while the other optical phonons are quite sensitive to the electrostatic intermolecular interactions. In table 3 it can be noticed that the frequencies of the Raman-active modes calculated for two values of the potential-function parameter C [set (1)], correspond to the experimental values found at 200 and 300 K. The polarization vectors indicate that the lower E_g mode is mostly librational while the higher E_g mode is mainly of translational character. As the translational displacement of molecules causes smaller changes in the dielectric susceptibility of the crystal than the librational displacements [24], we expect the lower E_g mode to give a much more intense band in Raman spectra than the higher-frequency mode. This qualitative prediction agrees with the experimental observations [22] and supports the assumed intermolecular potentials.

The polarization vectors of the E_g modes (which show that two inversion-related molecules perform "screw" movements along the x and y axes in opposite directions) indicate that the frozen pattern of these modes corresponds to the displacements of the s-triazine molecules in the low-temperature monoclinic phase, with respect to the trigonal structure. However, none of the E_g optical phonons behaves like a soft-mode and the amplitudes of these modes cannot be chosen as an order parameter of the phase transition. Nevertheless, these phonons are indirectly involved in a mechanism of the phase transition as "mediators" for translational–translational interactions. For this reason we shall calculate the static optical susceptibility [25] corresponding to the E_g modes:

$$\chi = \sum_{k,k'} \sum_{j \in E_g} \boldsymbol{Q}(kj)\, \boldsymbol{Q}(k'j)/\omega^2(j), \qquad (5)$$

where $\boldsymbol{Q}(kj)$ stands for the eigenvector components of the jth E_g mode with frequency $\omega(j)$, corresponding to the kth molecule in the unit cell.

For symmetry reasons the susceptibility decouples into purely rotational (R) and translational (T) parts, both being diagonal in the orthogonal axes system x, y, z. The calculated values are

$$\chi^{R}_{xx} = \chi^{R}_{yy} = (148.8\ \mathrm{kJ/mol})^{-1},$$

$$\chi^{T}_{xx} = \chi^{T}_{yy} = (234.0\ \mathrm{kJ/mol})^{-1},$$

for set (1) of the potential-function parameters. It is worth noticing that 90% of the rotational susceptibility is due to the contribution of the lowest E_g mode, which is mostly librational in character, while the translational susceptibility is mostly determined (70%) by the higher E_g mode.

3.2. Long-wave acoustic phonons

The acoustic phonons are the most important excitations in the high-temperature phase of s-triazine in the context of the phase transition, as the trigonal phase becomes unstable with respect to some of them. It has been found experimentally [5,7] that transverse acoustic phonons propagating in the $[q_x, 0, 0]$ and $[0, 0, q_z]$ directions become soft as the transition temperature is approached from above. The softening of the acoustic phonons is understood here as a tendency of the corresponding sound velocity to decrease to zero as the phase-transition temperature is approached. The strain component, $e_{\alpha\beta}$, generated by an acoustic phonon in the limit of long waves is given by [13]

$$e_{\alpha\beta} = \lim_{q_\beta \to 0} \mathrm{i}\, q_\beta\, Q_\alpha(q_\beta), \tag{6}$$

where $Q_\alpha(q_\beta)$ is an acoustic-mode amplitude with eigenvector polarized in the α direction and wavevector in the β direction. From this relation it is clear that the strain component is a macroscopic representation of the acoustic-mode amplitude. So the macroscopic strain, as an observable, will play the role of an order parameter for the structural phase transition rather than the acoustic-mode amplitude which is a microscopic quantity. In the trigonal phase of the s-triazine crystal, the strain components $e_{xz} = e_{yz} = e_4$ can be uniquely related to the amplitudes of the doubly degenerate transverse acoustic phonons propagating in the $[0, 0, q_z]$ direction and polarized in the x and y directions.

As a molecular crystal is not in fact an elastic continuum but has a discrete molecular structure with molecular degrees of freedom, the macroscopic strain, **e**, is accompanied by internal strains [25]. Now, let us analyze the internal strains corresponding with the e_4 strain produced by the soft acoustic phonon of Λ_3 symmetry ($[0, 0, q_z]$ direction in the Brillouin zone). We start with the harmonic potential energy of the crystal, written in terms of the dynamical-matrix elements:

$$V_{\mathrm{h}} = \tfrac{1}{2} \sum_{q} \sum_{k,k'} \sum_{ij} \sum_{\alpha\beta} D^{ij}_{\alpha\beta}(\boldsymbol{q}, kk') \times u^{i}_{\alpha}(\boldsymbol{q}, k)\, u^{j}_{\beta}(-\boldsymbol{q}, k'). \tag{7}$$

The indices k, k' denote sublattices; α, $\beta = x, y, z$ and $i, j = \mathrm{T}, \mathrm{R}$ are used to distinguish submatrices of the dynamical matrix which couple translational (T) and rotational (R) displacements of a molecule, $\boldsymbol{u}$. For the wave-vector directed along the hexagonal axis c (the Λ direction), the energy can be decoupled into parts corresponding to particular phonon symmetries. The twelve dispersion curves in this direction are classified as: $2\,\Lambda_1 + 2\,\Lambda_2 + 4\,\Lambda_3$ with Λ_3 being a two-dimensional representation. As the transverse acoustic phonons, which produce the e_4 strain and show an anomalous dispersion [7], form a doubly degenerate mode of Λ_3 symmetry (as well as three optical branches), we have to separate that part of the crystal energy which corresponds to this symmetry. This is easily done by means of projection operators which lead to a new set of coordinates:

$$\begin{aligned}
s_\alpha(\boldsymbol{q}) &= 2^{-1/2}\left[u^{\mathrm{T}}_\alpha(\boldsymbol{q}, 1) + u^{\mathrm{T}}_\alpha(\boldsymbol{q}, 2)\right],\\
w_\alpha(\boldsymbol{q}) &= 2^{-1/2}\left[u^{\mathrm{T}}_\alpha(\boldsymbol{q}, 1) - u^{\mathrm{T}}_\alpha(\boldsymbol{q}, 2)\right],\\
R_\alpha(\boldsymbol{q}) &= 2^{-1/2}\left[u^{\mathrm{R}}_\alpha(\boldsymbol{q}, 1) + u^{\mathrm{R}}_\alpha(\boldsymbol{q}, 2)\right],\\
P_\alpha(\boldsymbol{q}) &= 2^{-1/2}\left[u^{\mathrm{R}}_\alpha(\boldsymbol{q}, 1) - u^{\mathrm{R}}_\alpha(\boldsymbol{q}, 2)\right],
\end{aligned} \tag{8}$$

for $\alpha = x, y$. Now, the contribution to the crystal energy corresponding to the irreducible representation Λ_3 contains two parts with identical eigenvalues and for the further discussion we can use only one of them, reducing the problem to a four-dimensional one. This corresponds to taking one of two blocks assigned to the Λ_3 representation from the block-diagonalized dynamical matrix

(7) for a wave-vector in the [0, 0, q_z] direction. The eigenvalues of the Λ_3 modes are determined by the secular equation

$$\left[\mathbf{G}(q_z) - \omega^2\mathbf{M}\right] V(q_z) = 0, \tag{9}$$

where

$$\mathbf{G}(q_z) = \begin{bmatrix} a_+ & b & A_+ & B_+ \\ b^* & a_- & B_- & A_- \\ A_+ & B_-^* & \alpha_- & \delta \\ B_+^* & A_- & \delta^* & \alpha_+ \end{bmatrix}, \tag{10}$$

with elements being a linear combination of the dynamical matrix terms:

$$\begin{aligned} a_\pm &= D_{xx}^{TT}(q, 11) \pm D_{xx}^{TT}(q, 12), \\ b &= -\mathrm{i} D_{xy}^{TT}(q, 11), \\ A_\pm &= D_{xx}^{TR}(q, 11) \pm D_{xx}^{TR}(q, 12), \\ B_\pm &= -\mathrm{i}\left[D_{xy}^{TR}(q, 11) \pm D_{xy}^{TR}(q, 12)\right], \\ \alpha_\pm &= D_{xx}^{RR}(q, 11) \pm D_{xx}^{RR}(q, 12), \\ \delta &= -\mathrm{i} D_{xy}^{RR}(q, 11), \end{aligned} \tag{11}$$

and four-component vector $V(q_z) = [s_x, w_y, P_x, R_y]$. The set of equations (9) has four solutions, $\omega^2(q_z j)$ with corresponding eigenvectors, $\boldsymbol{Q}(q_z j)$. Then, we have the following relation:

$$\left[\mathbf{G}(q_z) - \omega^2(q_z j)\mathbf{M}\right] \boldsymbol{Q}(q_z j) = 0, \tag{12}$$

which can also be written in the form

$$\left[\mathbf{G}(q_z) - \omega^2\mathbf{M}\right]^{-1} = \sum_j \frac{\boldsymbol{Q}(q_z j)\boldsymbol{Q}(-q_z j)}{\omega^2(q_z j) - \omega^2}. \tag{13}$$

For $q_z = 0$, diagonalization of matrix $\mathbf{G}$ gives one acoustic mode of E_u symmetry, with $\omega = 0$ and eigenvector $\boldsymbol{Q}(0) = [s_x, 0, 0, 0]$ and three optical modes ($E_u + 2\ E_g$) determined by eigenvectors and eigenvalues of the matrix:

$$\mathbf{G}(0) = \begin{bmatrix} a_- & 0 & A_- \\ 0 & \alpha_- & 0 \\ A_- & 0 & \alpha_+ \end{bmatrix}, \tag{14}$$

as specified in table 3.

For the transverse acoustic phonon in the limit of long waves, eq. (12) can be solved by the perturbation method [26], using the expansions

$$\begin{aligned} \mathbf{G}(q_z) &= \mathbf{G}(0) + \mathbf{G}^{(1)} q_z + \mathbf{G}^{(2)} q_z^2 + \cdots, \\ \omega_{TA}(q_z) &= (\partial\omega/\partial q_z) q_z + \cdots = v_{TA} q_z + \cdots, \\ \boldsymbol{Q}(q_z) &= \boldsymbol{Q}(0) + \boldsymbol{Q}^{(1)} q_z + \cdots. \end{aligned} \tag{15}$$

Substituting these expansions one obtains [26]

$$\begin{bmatrix} a_+^{(2)} q_z^2 - v_{TA}^2 q_z^2 m & -\mathrm{i}\mathbf{G}^{(1)} q_z \\ \mathrm{i}\tilde{\mathbf{G}}^{(1)} q_z & \mathbf{G}(0) \end{bmatrix} \begin{pmatrix} s_x \\ \boldsymbol{Q}^{(1)} q_z \end{pmatrix} = \begin{pmatrix} 0 \\ 0 \end{pmatrix}, \tag{16}$$

where

$$a_+^{(2)} = \tfrac{1}{2} \lim_{q_z \to 0} \partial^2 a_+(q_z)/\partial q_z^2,$$

and the single-row matrix $\mathbf{G}^{(1)} = [b^{(1)}\ \ 0\ \ B_+^{(1)}]$ has elements

$$G_{\alpha\beta}^{(1)} = -\mathrm{i} \lim_{q_z \to 0} \partial G_{\alpha\beta}(q_z)/\partial q_z.$$

v_{TA} determines the velocity of the transverse acoustic phonon with the eigenvector $\boldsymbol{Q} = [s_x, \boldsymbol{Q}^{(1)} q_z]$ in the long-wave limit. It follows that

$$\boldsymbol{Q}^{(1)} q_z = -\mathrm{i}[\mathbf{G}(0)]^{-1} \tilde{\mathbf{G}}^{(1)} q_z s_x \tag{17}$$

and

$$v_{TA}^2 = m^{-1}\left\{ a_+^{(2)} - \mathbf{G}^{(1)}[\mathbf{G}(0)]^{-1}\tilde{\mathbf{G}}^{(1)} \right\}. \tag{18}$$

From eq. (13), $[\mathbf{G}(0)]^{-1}$ can be recognized as the static optical susceptibility, χ, with elements $\chi_{yy}^R(E_g)$, $\chi_{yy}^T(E_g)$ [both calculated in the previous section, see eq. (5)] and $\chi_{xx}^R(E_u) = 1/\alpha_-$. The components of the vector, $\boldsymbol{Q}^{(1)} q_z$, which determines internal strains induced by the external one,are given explicitly by

$$w_y^0 = \chi_{yy}^T b^{(1)} e_4, \tag{19}$$

$$R_y^0 = \chi_{yy}^R B_+^{(1)} e_4, \tag{20}$$

where the product $-\mathrm{i} q_z s_x$ in eq. (17) has been identified as the $e_4 = e_{xz}$ strain component. It can be seen that the $\boldsymbol{Q}^{(1)} q_z$ vector transforms according to the E_g representation as does the e_4 strain component. We can conclude therefore, that the shear strain is a measure of part of the transverse acoustic-phonon amplitude, while the internal

strains determined by eqs. (19) and (20) correspond to the second part of this amplitude. Within the harmonic approximation the internal strains are strictly proportional to the shear strain, e_4. The internal strains, induced by the low-frequency transverse acoustic phonon in the limit $q_z \to 0$, should not be confused with the amplitudes of the optical E_g modes, which are of much higher frequency, and none of the latter become soft at the transition temperature. In this sense, eq. (10) of ref. [9] is not correct as there is no condensation of any optical mode.

When eq. (18) is rewritten in an explicit form one obtains

$$v_{\mathrm{TA}}^2 = m^{-1}\left[a_+^{(2)} - b^{(1)}\chi_{yy}^{\mathrm{T}} b^{(1)} - B_+^{(1)}\chi_{yy}^{\mathrm{R}} B_+^{(1)}\right], \quad (21)$$

and the result can be interpreted as follows. The effective translational–translational interactions which determine the sound velocity are composed of direct translational–translational interactions (the first term) and indirect ones (the last two terms). These indirect interactions are determined by translational–rotational coupling and the rotational susceptibility. As the susceptibility is determined by optical-phonon frequencies and their eigenfunctions, one can say that the optical phonons play a role of mediators for the effective translational interactions in the crystal. The elastic constant, c_{44}, determined by the sound velocity v_{TA} from eq. (21), is

$$c_{44} = c_{44}^0 - v^{-1}\left[b^{(1)}\chi_{yy}^{\mathrm{T}} b^{(1)} - B_+^{(1)}\chi_{yy}^{\mathrm{R}} B_+^{(1)}\right], \quad (22)$$

where the "bare" elastic constant c_{44}^0 is determined by the direct translational–translational interactions. The effect of indirect interactions on sound velocities and elastic constants can be seen from the results presented in table 4, which follow from calculations with set (1) of potential-function parameters. As a result of the competition between direct and indirect interactions, the acoustic phonon TA becomes soft, causing a violation of the stability condition, $c_{44} > 0$, which is observed in the temperature dependence of the elastic constant [5].

4. Phase transition

The above considerations, concerning renormalization of the transverse acoustic phonon and the corresponding elastic constant, show that even within the harmonic approximation it is possible to explain an instability of the high-temperature structure of s-triazine. If the elastic constant c_{44} decreases to zero, the crystal may distort continuously to a new structure with symmetry determined by the e_4 strain component and the accompanying internal strains: translation, w_y^0, and rotation, R_y^0 of the molecules. It will be shown in the next section, that it follows from calculations that the molecular translational displacements, although in principle possible, are found to be very small; they have not been deduced from recent experiments [27]. Thus, it seems to be reasonable to neglect the translational internal strain in all further considerations concerning the phase transition (the same approximation has been used in

Table 4
Sound velocities (in 10^3 m/s) and effective elastic constants (in 10^9 N/m^2) as calculated for the trigonal structure of s-triazine [with parameter set (1)], which is close to the experimental structure at 300 K

Propagation	$[q_x, 0, 0]$			$[0, 0, q_z]$	
Mode	T_1	T_2	L	T	L
velocity					
bare	1.495	3.094	4.042	1.360	3.770
effective	0.927	1.970	3.766	1.049	3.630
elastic constants	c_{11}	c_{33}	c_{44}	c_{12}	c_{14}
	20.08	18.63	1.95	9.78	1.17

previous theories, without explanation). Within this approximation the interesting part of the harmonic crystal energy density is

$$V_{\mathrm{h}} = \tfrac{1}{2}c_{44}^{0}e_4^2 + Ae_4R_y + \tfrac{1}{2}aR_y^2, \tag{23}$$

where the following substitutions have been used: $R_y = R_y^0$, $A = -v^{-1}B_+^{(1)}$, $a = (\chi_{yy}^{\mathrm{R}})^{-1}$, for a unification of the notation with that used by Raich and Bernstein [8]. Using the corresponding equilibrium conditions, eq. (23) can be rewritten as

$$V_{\mathrm{h}} = \tfrac{1}{2}\left(c_{44}^{0} - A^2/a\right)e_4^2 = \tfrac{1}{2}c_{44}e_4^2, \tag{24}$$

with c_{44} being the effective elastic constant within the approximation that neglects the translational internal strain.

So far, we have discussed that part of the s-triazine crystal energy which is expected to change during the phase transition, still within the harmonic approximation. To discuss the phase transition, one has to go beyond this approximation for two reasons: in order to stabilize a new structure which is expected as a result of the high-temperature phase instability and to explain the slight first-order character of the transition. The internal energy of the crystal can be written in terms of e_4 and R_y (both transforming according to the $\mathrm{E_g}$ representation of the factor group of the high-temperature phase) as a series [8]:

$$V = \tfrac{1}{2}c_{44}^{0}e_4^2 + Ae_4R_y + \tfrac{1}{2}aR_y^2 + \tfrac{1}{3}bR_y^3 + \tfrac{1}{4}dR_y^4 + \tfrac{1}{2}Ke_4R_y^2 + \tfrac{1}{2}Ee_4^2R_y + \cdots, \tag{25}$$

which can be seen as an anharmonic generalization of eq. (23). It has to be emphasized that here R_y is the slow rotational variable which follows the strain e_4, according to the previous considerations; it should not be confused with an optical-phonon coordinate.

In order to calculate an equilibrium configuration for the crystal, one has to add the entropy term to the internal energy. We follow the arguments of Raich and Bernstein [8] and write

$$-TS/N = -CT + k_{\mathrm{B}}TR_y^2 + \cdots, \tag{26}$$

where C is a constant. This expression represents the leading terms in an expansion of the configurational entropy in terms of the slow rotational variable, associated with the soft acoustic phonon. When adding the entropy term to the internal energy (25), it makes the rotational-susceptibility temperature dependent and the substitution

$$a = a_0(T - T_0), \tag{27}$$

can be made, with a_0 and T_0 as adjustable parameters. The inverse of the rotational susceptibility calculated from optical-phonon frequencies in section 3 has to be taken for the value of a at $T = 300$ K, since the equilibrium structure for which it has been calculated was close to the experimental one at that temperature.

When eq. (27) is substituted into eq. (25), the latter represents an anharmonic expansion of the free energy. It has to be emphasized that it contains only that part of the energy which is associated with the soft acoustic phonon and the two variables, e_4 and R_y, are only formally specified separately. These variables are closely related by the equilibrium condition

$$R_y = -(A/a)e_4 + (KA/a^2 - E/2a)e_4^2 + \cdots, \tag{28}$$

where the first term reproduces the lattice dynamical result, within the harmonic approximation, and the non-linear terms follow from anharmonicity of the crystal and not, as assumed by Rae [9], from consideration of a corresponding optical mode.

By introducing eq. (28) into (25) the free energy is written in terms of the e_4 strain component only (see eq. (23) in ref. [8]) and the effective elastic constant

$$c_{44} = c_{44}^{0} - A^2/a_0(T - T_0) \tag{29}$$

is found. At temperature $T = T_0'$, the indirect translational–translational interactions (determined by the translational–rotational coupling constant, A, and the temperature-dependent rotational susceptibility) overcome the direct interactions which determine the "bare" elastic constant, and c_{44} goes to zero. This is a macroscopic manifestation of the softening of the transverse acoustic phonon. As a result of this softening, the slow variables, e_4 and R_y, accompanied with the phonon become static and the deformation of the unit cell (according to e_4 strain) and molecular tilt

(according to the internal strain R_y) occur. The low-temperature phase represents, therefore, the frozen pattern of the transverse acoustic phonon. Details of the thermodynamical analysis of the free-energy expansion can be found in ref. [8].

5. The low-temperature phase

The low-temperature, monoclinic phase has been numerically simulated according to the view developed that the structure is a result of the condensation of the transverse acoustic phonon. The trigonal, high-temperature unit cell has been deformed according to e_4 strain, i.e. the monoclinic angle β_m has been assumed as

$$\beta_m = \mathrm{ctg}^{-1}\left(e_4 + \mathrm{ctg}\,\beta_m^0\right), \tag{30}$$

for a given strain, and the lattice constant a_m^0 has been changed to the value

$$a_m = a_m^0 \sin\beta_m^0 / \sin\beta_m, \tag{31}$$

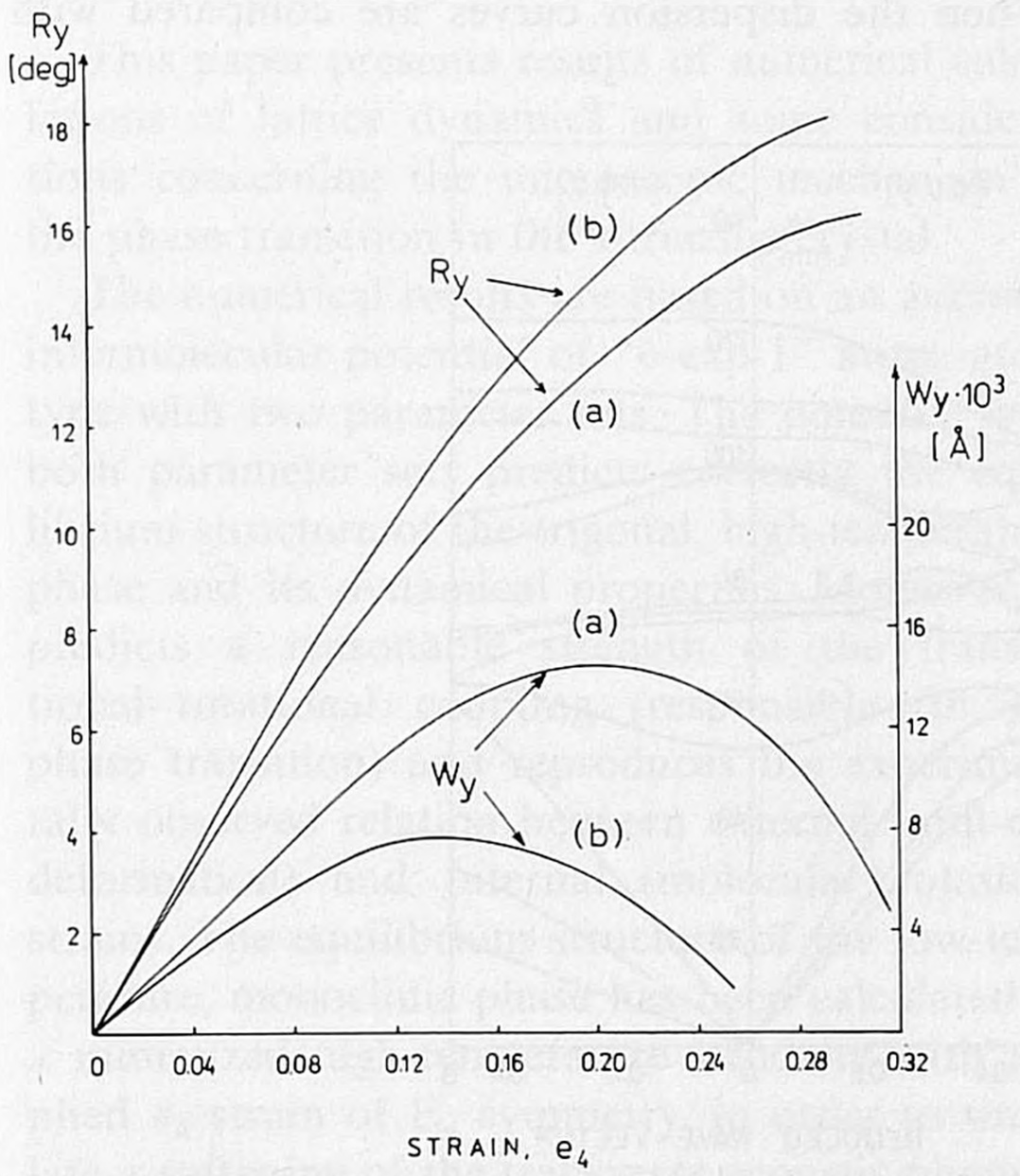

Fig. 3. Calculated shear strain (e_4) dependence of internal strains: molecular rotation (R_y) and translation (w_y) calculated for parameter set (1) [curve (a)] and set (2) [curve (b)] of the potential function.

to ensure zero strain e_1 [15]. The other lattice constants were kept at the values found for the trigonal phase. For the given lattice parameters (corresponding to an assumed strain e_4) the crystal energy has been minimized with respect to molecular rotations R_y and translations w_y (the internal strains). The calculated internal strains can be seen as a response of the molecular configuration to an applied external strain e_4, in order to compensate for an increase in the crystal energy introduced by the unit-cell deformation.

As it follows from the previous considerations, the relation between internal and external strains is expected to be linear for small e_4 strains and this is confirmed by our calculations. Fig. 3 shows the dependence of the molecular rotation R_y and translational displacement on the applied external strain. The translational displacement is found to be very small and shows an intriguing strain dependence. The calculations indicate that very precise crystallographic measurements would be required to detect the translational internal strain in the s-triazine crystal; the assumption to neglect this contribution in the free-energy expansion is fully justified.

The calculated strain dependence of molecular rotations (shown in fig.3) can be represented by the following functions:

$$R_y = 1.42\,e_4 - 1.36\,e_4^2, \quad \text{set (1)},$$

$$R_y = 1.48\,e_4 - 1.01\,e_4^2, \quad \text{set (2)}, \tag{32}$$

where R_y is measured in radians. These functions can be compared with the experimentally found relation [9]

$$R_y = 1.40\,e_4 + 2.62\,e_4^2,$$

assuming an identification of e_4 with $\tan\theta \approx \theta$ (in the notation of ref. [9]). From this comparison it is concluded that the potential function assumed for the s-triazine crystal (with either set of parameters) predicts the translational–rotational coupling strength very well, within the linear approximation. The difference in the quadratic term should not be considered as very significant since this term gives a non-negligible contribution only for strains greater than 15%, which corresponds to the

monoclinic structure far from the phase-transition temperature.

When the relation (28) is introduced into eq. (25), the crystal energy is expressed in terms of external strain only and the effective elastic (translational) potential has the form

$$V = 86.7\, e_4^2 - 149.0\, e_4^3 + 1205.0\, e_4^4\ [\mathrm{kJ/mol}]. \quad (33)$$

The first term of this effective potential yields the effective elastic constant c_{44} ($c_{44} = 1.95 \times 10^9$ $\mathrm{N/m^2}$). Any further analysis of the effective crystal potential requires knowledge of the parameters a_0 and T_0 introduced by relation (27). These parameters cannot be obtained from our calculations, however, they can be fitted to experimental data as done by Raich and Bernstein [8]. From semi-quantitative estimates, we can only conclude that the effective elastic energy (33), calculated from the assumed intermolecular potential for the s-triazine crystal, gives too weak an anharmonicity for predicting correctly all thermodynamic effects of the phase transition (the temperature of the transition, in particular). The potential, however, does predict properly the strength of the translational–rotational coupling which is the driving force for the transition.

Having determined equilibrium structures of the low-temperature monoclinic phase for different applied strain values, e_4, the lattice dynamics at these structures has been calculated within the conventional harmonic approximation. Frequencies of all optical phonons as a function of the strain are plotted in fig. 4. The A_g–B_g splitting for the lowest (trigonal phase) E_g mode can be described by the relation

$$\Delta(\omega^2) = 7100\, e_4 + 19100\, e_4^2\ (\mathrm{cm^{-1}})^2,$$

and it agrees well with the experimental dependence described by Rae [9], but again only for the linear term. The quadratic term is found to be much smaller; the difference can be due to a temperature effect (not taken into account in the present calculations) and possibly also to the fitting procedure applied by Rae [9], which has been commented on by Raich et al. [10].

Finally, the phonon dispersion curves for two symmetry directions in the monoclinic phase have

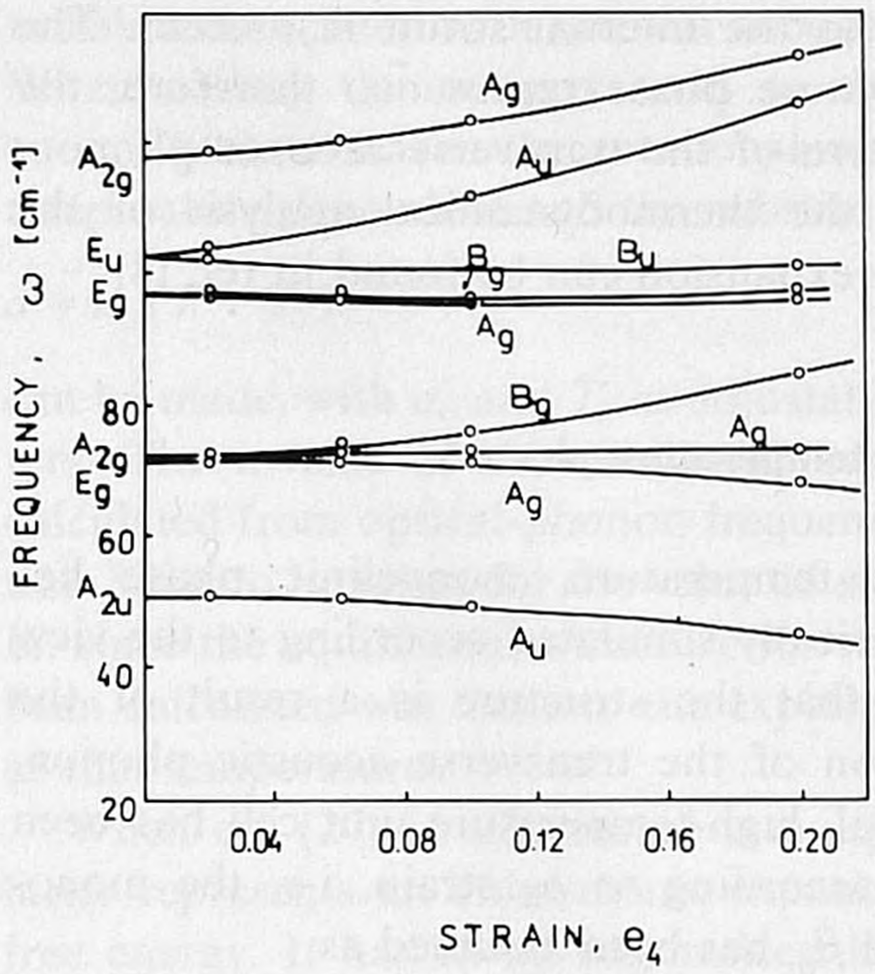

Fig. 4. Calculated [set (1)] shear strain (e_4) dependence of the nine zone-center optical-phonon frequencies; the assignments correspond to the trigonal phase at $e_4 = 0$ and to the monoclinic phase at $e_4 \neq 0$.

been calculated. Fig. 5 shows these curves, calculated for the equilibrium structure corresponding to the strain $e_4 = 0.06$ [with parameter set (1)]. When the dispersion curves are compared with

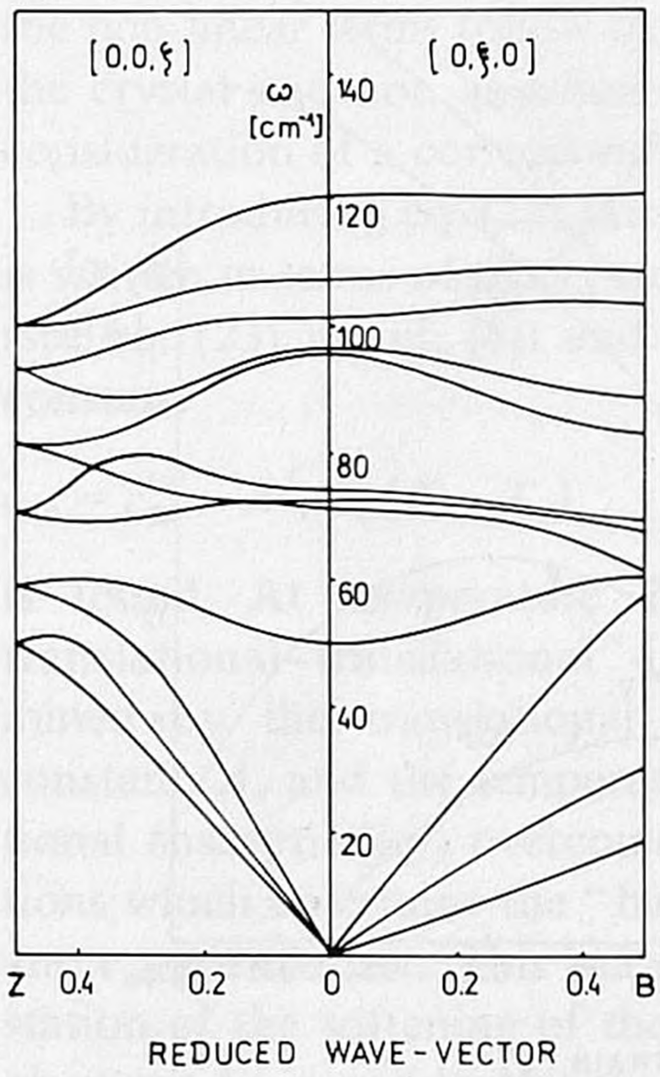

Fig. 5. Phonon-dispersion curves for two symmetry directions of the monoclinic phase of s-triazine. The calculations [with parameter set (1)] are performed for the deformed trigonal phase with $e_4 = 0.06$ (see text for details).

those for the trigonal phase (fig. 2), one observes a pronounced effect of the elastic strain on the dispersion curves; in particular, a "compression" of the phonon energies at the zone-boundary point $(0, 0, \frac{1}{2})$ is found. It is believed that these calculations of the dispersion curves for both phases of the s-triazine crystal will be helpful for a better understanding of the Raman spectra of the crystal, especially in the vicinity of the phase-transition temperature. Strong coupling between optical and soft acoustic phonons is expected, which could lead to "strain-induced" spectra. Due to the coupling, a kind of second-order Raman effect can occur and the spectra for non-active polarizations can be seen as a density of phonon states (which could be calculated from the presented dispersion curves). Preliminary experimental results do show such an effect [28] and a detailed analysis of the Raman spectra from the point of view of translational–rotational interactions is a task for the future.

6. Conclusions

This paper presents results of numerical calculations of lattice dynamics and some considerations concerning the microscopic mechanism of the phase transition in the s-triazine crystal.

The numerical results are based on an assumed intermolecular potential of "6-exp-1" atom–atom type with two parameter sets. The potential with both parameter sets predicts correctly the equilibrium structure of the trigonal, high-temperature phase and its dynamical properties. Moreover, it predicts a reasonable strength of the translational–rotational coupling (responsible for the phase transition) and reproduces the experimentally observed relation between external (unit-cell deformation) and internal (molecular rotation) strains. The equilibrium structure of the low-temperature, monoclinic phase has been calculated as a minimized high-temperature structure with applied e_4 strain of E_g symmetry, in order to simulate a softening of the transverse acoustic phonon.

Conclusions concerning the microscopic mechanism of the ferroelastic phase transition are the following. The transition from the trigonal to the monoclinic phase is a result of instability of the high-temperature phase with respect to the doubly degenerate transverse acoustic phonon of Λ_3 symmetry in the $[0, 0, q_z]$ direction. In the long-wave limit, this acoustic phonon, when it becomes soft, produces the static shear strain, e_4, of E_g symmetry which is followed by "screw" displacements of the molecules of the same symmetry, called internal strains. The frequency of this phonon, and also its velocity [see eq. (21)], is determined by competition between direct translational–translational and indirect interactions. The latter depend on the strength of the translational–rotational coupling and on the (rotational) optical susceptibility (13). Both quantities are reasonably well predicted by the assumed potential. The role of translational–rotational coupling in the s-triazine crystal is to affect the optical phonons and to couple them to the acoustic phonon. Thus, the optical phonons are mediators for the indirect translational–translational interactions which compete with the direct ones. It is reasonable to assume that the optical susceptibility is temperature dependent, which leads to an increase of the indirect interactions at lower temperature. At some temperature they overcome the direct translational crystal field and cause a condensation of the long-wave transverse acoustic phonon, i.e. a structural transformation. The molecular (almost purely rotational) displacements can be seen as a response of the molecules to the shear strain, in order to optimize the effective response of the crystal to the unit-cell deformation. It has been shown that within the harmonic approximation there is a strictly linear dependence between the internal and shear strains. Also this relation depends on the translational–rotational coupling and the optical susceptibility; for E_g symmetry the latter can be partitioned into translational and rotational contributions.

In general, a non-linear dependence between shear and internal strains follows from the anharmonicity of the crystal potential and cannot be justified by eq. (10) of ref. [9], which is derived within the harmonic approximation. The conclusion from paper [9] that the condensation of the acoustic mode is accompanied by condensation of the corresponding optical mode, is not correct. There is no condensation of any optical mode at

the phase-transition temperature.

The microscopic mechanism of the phase transition presented here differs also from that given by Raich and Bernstein [8]. These authors concluded, just as we did, that the transition arises from a coupling between the transverse acoustic mode (the soft one) and molecular rotations, via translational–rotational interactions. They suggest, however, that the structural instability is due to a competition between direct and indirect orientational interactions.

Summarizing, we wish to emphasize once more that in our model the softening of the acoustic phonon mode, which corresponds with the phase transition, is due to the competition between direct and indirect translational couplings. The optical phonons enter only into the latter by determining the optical (rotational) susceptibility. This does not imply that the softening of this particular acoustic mode "causes" the phase transition. Our model, as well as the other ones, is only intended to explain the experimentally observed behaviour.

Acknowledgement

We thank Dr. K. Pesz for helpful discussions. This work was partially supported by the Polish Academy of Sciences within the Mr.I.9 project.

References

[1] B. de Raedt, K. Binder and K.H. Michel, J. Chem. Phys. 75 (1981) 2977;
D. Sahu and S.D. Mahanti, Phys. Rev. B26 (1982) 2981.
[2] S. Haussühl, Solid State Commun. 13 (1973) 147;
J.M. Rowe, J.J. Rush, N.J. Chesser, K.H. Michel and J. Naudts, Phys. Rev. Letters 40 (1978) 455;
A. Loidl, K. Knorr, J. Daubert, W. Dultz and W.J. Fitzgerald, Z. Physik B38 (1980) 153.
[3] M. Julian and F. Lüty, Ferroelastics 16 (1977) 201;
S.K. Satija and C.H. Wang, Solid State Commun. 28 (1978) 617;
J.M. Rowe, J.J. Rush, D.J. Hinks and S. Susman, Phys. Rev. Letters 43 (1979) 1158;
J.Z. Kwiecien, R.C. Leung and C.W. Garland, Phys. Rev. B23 (1981) 4419.
[4] K.H. Michel and J. Naudts, J. Chem. Phys. 68 (1978) 216.
[5] A. Yoshihara, C.L. Pan, E.R. Bernstein and J.C. Raich, J. Chem. Phys. 76 (1982) 3218.
[6] A. Yoshihara, W.D. Wilber, E.R. Bernstein and J.C. Raich, J. Chem. Phys. 76 (1982) 2064;
A. Yoshihara, E.R. Bernstein and J.C. Raich, J. Chem. Phys. 77 (1982) 2768.
[7] I.U. Heilman, W.D. Ellenson and J. Eckert, J. Phys. C12 (1979) L185.
[8] J.C. Raich and E.R. Bernstein, J. Chem. Phys. 73 (1980) 1955.
[9] A.I.M. Rae, J. Phys. C15 (1982) 1883.
[10] J.C. Raich and E.R. Bernstein, J. Phys. C15 (1982) L283; A.I.M. Rae, J. Phys. C15 (1982) L287.
[11] J.C. Raich, E.R. Bernstein and A. Yoshihara, Chem. Phys. Letters 82 (1981) 138.
[12] J.C. Raich, E.R. Bernstein and A. Yoshihara, Mol. Phys. 45 (1982) 197.
[13] R.A. Cowley, Advan. Phys. 29 (1980) 1.
[14] J.H. Smith and A.I.M. Rae, J. Phys. C11 (1978) 1761, 1771.
[15] J.L. Schlenker, G.V. Gibbs and M.B. Boisen Jr., Acta Cryst. A34 (1978) 52.
[16] F. Mulder, G. van Dijk and C. Huiszoon, Mol. Phys. 38 (1979) 557, 1497.
[17] A.I.M. Rae, J. Phys. C11 (1978) 1779.
[18] P.F. Price, E.N. Maslen and W.T. Delaney, Acta Cryst. A34 (1978) 194.
[19] F. James and M. Ross, Program MINUIT, CERN Computer Centre Program Library, D506, D516.
[20] G.E.W. Bauer and C. Huiszoon, Mol. Phys. 47 (1982) 565.
[21] Z. Gamba and H. Bonadeo, J. Chem. Phys. 75 (1981) 5059.
[22] G.R. Elliot and Z. Iqbal, J. Chem. Phys. 63(1975) 1914.
[23] S.J. Daunt, H.F. Shurvell and L. Pazdernik, J. Raman Spectry. 4 (1975) 205.
[24] T. Luty, A. Mierzejewski and R.W. Munn, Chem. Phys. 29 (1978) 353.
[25] T. Luty and R.W. Munn, J. Phys. C15 (1982) 4459.
[26] T. Luty and I. Uszynski, J. Chem. Phys. 72 (1980) 1369.
[27] S.M. Prasad, A.I.M. Rae, A.W. Hewat and G.S. Pawley, J. Phys. C14 (1981) L929.
[28] H. Fountaine and A. Mierzejewski, private communication.